



Biomolecular materials: structure, interactions and higher order self-assembly

C.R. Safinya

Materials Department, Physics Department, Biochemistry and Molecular Biology Program, University of California, Santa Barbara, CA 93106, USA

Received 6 September 1996

Abstract

We review recent experimental work in two-dimensional (2D) membrane–protein assemblies, in lamellar fluid membrane phases containing tail anchored polymer–lipids, and in binary lipid mixtures which self-assemble into equilibrium tubular vesicle phases. We outline new directions in the development of technologically useful biomolecular materials. Synchrotron X-ray scattering studies of the purple membrane comprised of the 2D self-assembly of the membrane protein bacteriorhodopsin (bR) are described. In particular, experiments are described in the low humidity regime where a remarkable, exceedingly high temperature phase of bR has been discovered. Higher order self-assemblies of the stacked 2D membranes, achieved by water removal, result in the complete suppression of the melting transition, and the absence of protein denaturation up to 140°C. Aside from the scientific interest of elucidating the intraprotein and interprotein forces responsible for retaining the folded structure at high temperatures, the findings suggest methods for the development of “heat-proof proteins”. Higher order self-assemblies of functional proteins used in biosensors (e.g. toxin detectors), in bioreactors (purifying genetically engineered proteins with high temperature sieves) and in catalytic applications should be stabilized to high temperatures. In another series of experiments, we shall describe the properties of a new class of lamellar hydrogels based on fluid membranes which contain small amounts of single-end-anchored polymer–lipids. There are striking differences between these membrane-based liquid crystalline biogels labeled $L_{\alpha,g}$ and isotropic hydrogels of polymer networks; for example, mixtures with a larger water content require a smaller polymer concentration for gelation. A defining signature of these lamellar hydrogels is the presence of a highly defected underlying microstructure. “Bioactive gels” useful in tissue healing or drug delivery applications may be envisaged with activity derived from membrane-anchored peptides, proteins or other drug molecules, and mechanical stability resulting from the polymer–lipid minority component. © 1997 Elsevier Science B.V.

Keywords: Higher order self-assembly; Lamellar biogels; Lipids; Membrane proteins; Optical microscopy; Polymer–lipids; Tubular vesicles; X-ray diffraction and scattering

1. Introduction

In this paper we review a series of recent experiments which are aimed at elucidating the structure and self-assembling interactions in a variety of biomolecular materials and complex fluids systems. These include (1) stacked two-dimensionally self-

assembled integral-membrane–proteins, (2) multi-layer lipids containing membrane-anchored polymers and (3) multilayer membranes of mixed lipids. The material systems should have many technological consequences for the processing of advanced materials consisting of self-assembled macromolecular sheets and functionalized inter-

faces manipulated at the molecular level (e.g. using molecules that are optically active or have particular shapes for specific binding to ligands), to produce multilayered structures with tailored optical, high temperature enzymatic separations and sensor properties.

High resolution X-ray scattering studies of these important biological materials is now becoming feasible with the recent advent of dedicated high brightness synchrotron sources required for the structural studies of these weakly scattering biological materials. We stress that, compared with the vast experimental knowledge regarding lipid phase behavior, there are very few experimental data on membrane-associated protein and polymer phase behavior. To date, electron microscopy has been used as the primary structural probe of membrane-associated proteins, although at isolated points in the phase diagram, by using staining and freeze-etching techniques (see for example [1]). In-situ synchrotron-based high resolution diffraction and scattering techniques add unique information for the complete characterization of these complex materials including their global phase behavior, structural nature and intermacromolecular interactions, on length scales spanning Ångstroms to micrometres.

Synchrotron techniques (see for example [2–4]) of high resolution small- and wide-angle X-ray scattering are used for the in-situ determination of both structure and interactions [2,4] by measuring the material's elasticities (e.g. compression and shear moduli, and bending rigidities) derived from the intermembrane and intermacromolecular interactions. Synchrotron-based grazing-incidence X-ray scattering (GIXS) and grazing-incidence reflectivity (GIR) techniques (see for example [5–7]) may be used to characterize the structure of ultrathin overlayers on substrates. GIR allows one to measure the average electron density profile normal to the substrate, yielding the membrane film thickness and height roughness [6]. Additionally, by measuring the diffuse scattering around the specular reflection, the in-plane lateral roughness present in the electron density is probed [7]. This technique complements the GIXS technique used at synchrotron sources to characterize the in-plane structure of ultrathin membrane layers

deposited on a solid substrate [5]. In addition, as we shall show, because of the very large length scales some macromolecular self-assemblies can be directly imaged with optical microscopy.

2. Experimental details

2.1. Chemicals

Purple membrane (PM) (native two-dimensional (2D) hexagonal lattice of bacteriorhodopsin (bR)) was prepared as described in [8]. A lyophilized suspension of PM in distilled water (5 mg ml^{-1}) was centrifuged and 1 mg was spread on a thin, $25 \mu\text{m}$ (hydrophilically prepared), silicon wafer transparent to X-rays and covering an area with diameter about 10 mm. The wet membrane-substrate preparation was then placed in a closed container and brought into equilibrium with deionized water at about 100% relative humidity. This sample procedure yielded highly oriented multilayer samples approximately $10 \mu\text{m}$ thick with a mosaic spread of the layer normals of about 15° measured through a standard crystallographic “rocking-curve” X-ray scan. Dimyristoyl phosphatidyl choline (DMPC) and the polymer-lipid 1,2-diacyl-*sn*-glycero-3-phosphoethanolamine (DMPE)-*N*-[poly(ethylene glycol)] (PEG) at two different molecular weights of PEG, 2053 g mol^{-1} (PEG2000; $n=45$ is the degree of polymerization) and 5181 g mol^{-1} (PEG5000; $n=113$), were purchased from Avanti Polar Lipids, Inc. (Alabaster, AL).

2.2. Methods

The X-ray scattering and diffraction experiments were carried out with both an 18 kW rotating-anode X-ray generator and, at higher resolutions, the synchrotron sources at the National Synchrotron Light Source and the Stanford Synchrotron Radiation Laboratory. The optical micrographs were taken with a Nikon Diaphot 300 equipped for epifluorescence and high resolution differential interference contrast.

3. Results and discussion

3.1. Higher order self-assembly of the two-dimensional lattice of bacteriorhodopsin: structure, interactions and heat-proof proteins

Recently, Shen et al. [8] and Safinya and Rothschild [9] reported the discovery of an exceedingly high temperature stable phase of the membrane protein bR, in dry multilayers of the self-assembled 2D lattice, revealed through synchrotron X-ray scattering experiments. As we discuss later in this section, these experiments lead one to propose the development of a general class of more highly ordered self-assembled membrane-associated protein systems with potential high temperature stability of proteins and enzymes. Aside from the clear scientific interest of elucidating the intraprotein and interprotein forces responsible for retaining the folded protein structure at high temperatures, obtaining increased stability of biomolecular molecules, especially at high temperatures (i.e. heat-proof proteins), is also technologically important. High temperature proteins will undoubtedly find utility in numerous present-day and future biotechnology applications. For example, current PCR machines which cycle to high temperatures to denature DNA, utilize high temperature DNA polymerase enzymes derived from thermophile Archaeobacteria which have an optimal growth at 90°C [10]. Other examples where high temperature stability is desirable include biosensors (e.g. toxin detectors), in bioreactors, and high temperature catalysis. Before outlining our strategy we first briefly review the recent results on bR.

bR is a light-driven proton pump [11], responsible for the photosynthesis carried out by *Halobacterium halobium*. In its native form, bR self-assembles into a 2D crystalline PM which is incorporated into the lipid bilayer plane of the plasma membrane of the bacterium. Native PM has a diameter of the order of 0.5 μm and bilayer thickness of 49 Å; it consists of trimers of bR which self-assemble in a hexagonal lattice with a spacing of 61.6 Å with the remaining space filled by lipid (Fig. 1). By using cryoelectron microscopy Henderson and Unwin [12] showed that each bR molecule, shown schematically on the right of

Fig. 1, consists of a polypeptide chain which weaves back and forth through the membrane, forming seven-folded tube-like α -helical structures. The absorption of light by the PM, which in its light-adapted form has an absorption maximum near 570 nm, is due to retinal found also in the visual pigment rhodopsin (see for example [11,13]).

There are several features which make bR an attractive biomaterial; at low temperatures, bR can function as an optically driven bistable switch. Thus it may be possible to develop optically addressable materials containing mutant forms of bR [14] which function as high density memories and holographic media at room temperature [15].

Under fully hydrated conditions, the 2D lattice of bR undergoes a reversible melting transition around 70°C, followed by a broad denaturation transition starting at around 90°C [4,8] where the bR protein undergoes a transition from its tightly coiled α -helical conformation (Fig. 1), which is the biologically active form, to a more polymer-like random coil structure, where the characteristic 570 nm absorption band in the visible disappears [16].

As described by Shen et al. [8] the behavior under dry conditions is strikingly different. Fig. 2(a) shows plots of the X-ray intensity in dry multilayers under flowing nitrogen conditions, for scans along the in-plane membrane direction ((10), (11), (20), and (21) peaks) both at room temperature and at very high temperatures, $T=132^\circ\text{C}$. The multilayer structure is essentially unchanged as one goes from room temperature to high temperatures. Fig. 2(b) compares high resolution plots of the X-ray intensity under vacuum, for scans along the in-plane direction at $T=76^\circ\text{C}$ and 140°C . The observation of sharp in-plane peaks is quite remarkable and shows that, under dry conditions, the ordered hexagonal lattice remains intact to very high temperatures of the order of 140°C . Furthermore, the fact that the X-ray structure factor intensities are essentially unchanged from room temperature to 140°C indicates that bR remains in its tightly coiled α -helix conformation with bR trimers self-assembled in the hexagonal lattice. The order-disorder transition, which occurs at around $T=69^\circ\text{C}$ at high humidities [4,8],

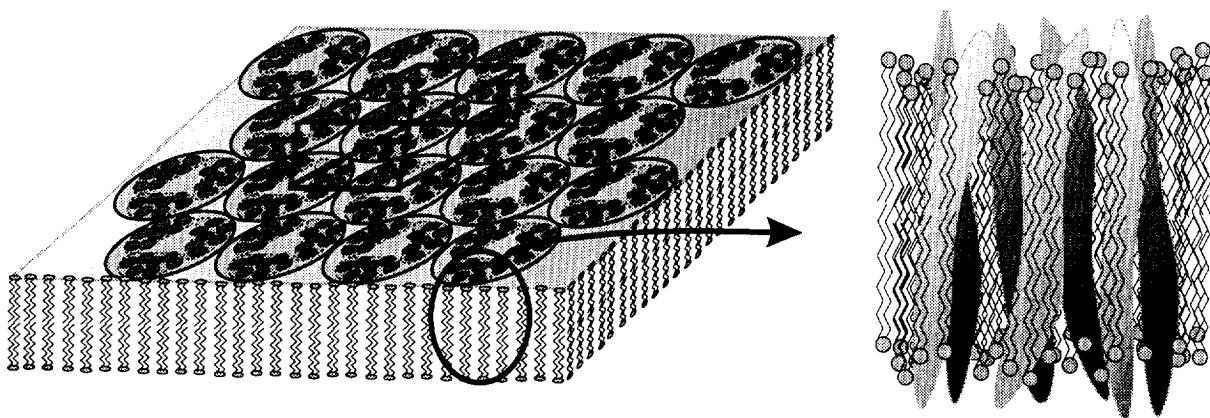


Fig. 1. Schematic top view of the hexagonal lattice of bR trimers with a magnification of a side view of one bR molecule showing the seven α -helices which span the PM.

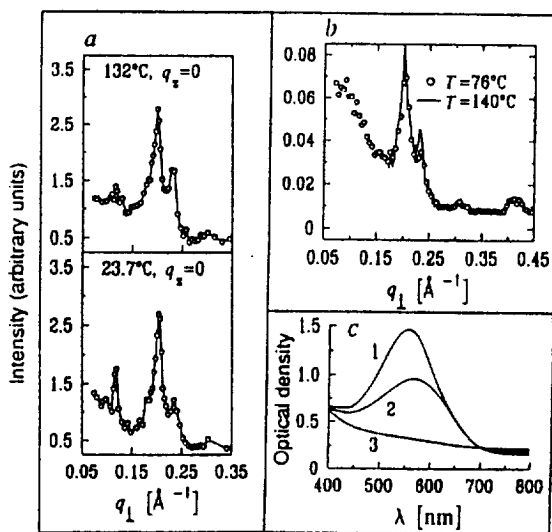


Fig. 2. Low humidity (dry), (a) low temperature and (b) high temperature X-ray and (c) absorption data from multilayers of bR showing that “higher order self-assemblies” of bR (through dehydration) result in the protein’s extreme high temperature stability as discussed in the text (from Shen et al. [8]).

is suppressed entirely under these dry conditions as the membrane bilayers are forced to stack in close proximity. The X-ray data [8] also show a complete lack of interlayer positional correlations under these dry conditions. Thus, the suppression of the in-plane melting transition is not a result of the lock-in of interlayer correlations and a crossover from 2D to three-dimensional (3D) behavior.

Fig. 2(c) shows the visible absorption spectrum of three dry PM samples measured at room temperature: curve 1 is for the sample at 23°C ($\lambda_{\text{max}} = 560 \text{ nm}$), while the other two samples were cycled through 140°C (curve 2; $\lambda_{\text{max}} = 567 \text{ nm}$), which resulted in a reduced intensity and a slight red shift, and 160°C (curve 3) which bleached the sample irreversibly (i.e. loss of retinal) and showed a flat visible band. The retention of the purple color characteristic of the absorption around 570 nm of all the high temperature and dehydrated samples held below $T = 140^\circ\text{C}$ indicates that the retinal molecule responsible for the absorption remains covalently attached and maintains its normal interaction with the protein. It is highly likely that the absence of the melting transition enhances the stability of the protein structure at this unusually high temperature of about 140°C.

This remarkable discovery suggests some interesting new directions. High temperature stability may be imparted to other proteins and enzymes through higher order self-assembly without the need for 3D crystallization. A broad range of temperature-stabilized ordered multilayered self-assemblies of proteins and enzymes may be envisaged which utilize the biotin-avidin scheme (Fig. 3(b)) pioneered by Uzgiris and Kornberg [17], involving the specific binding of macromolecules to a single functionalized interface.

Avidin is a water-soluble protein [18] which binds specifically via a lock-and-key interaction to

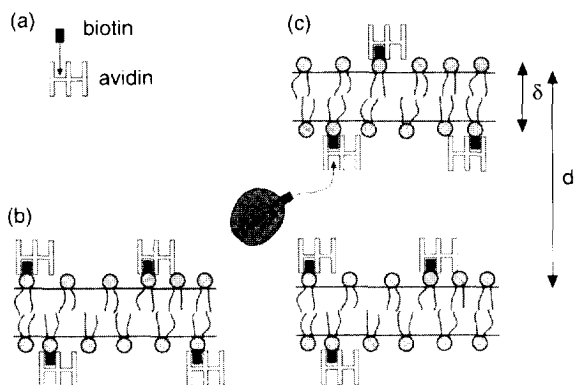


Fig. 3. (a) Affinity of biotin to avidin. (b) Single bilayer of lipid mixed with biotinylated lipid with bound avidin (c) Multilayers of (b). The functionalized bilayer in (b) and multilayers in (c) are capable of binding any biotinylated macromolecule (e.g. proteins, peptides or nucleic acids shown in (c)).

biotin (vitamin H) and its homologues (Fig. 3(a)). Single bilayers have been prepared on substrates consisting of a mixture of biotinylated lipid and lipid, and shown [17,19] to bind the ligand avidin specifically (Fig. 3(b)). Because avidin possess four binding sites for biotin, two on either side of the molecule, the avidin-covered membrane (bound to the biotinylated lipid) itself becomes the receptor for the ligand biotin or any other biotinylated macromolecule (shown in Fig. 3(c)). The real significance of the avidin-coated system lies in the fact that, through straightforward synthesis, many macromolecular materials can be biotinylated [19].

In our laboratory we are exploring the extension of this scheme to multilayers shown schematically in Fig. 3(c) which should result in high temperature proteins and enzymes. Aside from the search for high temperature proteins, these experiments are also designed to characterize protein–protein interactions. Very little is known about the protein–protein and protein–membrane interactions in real experimental cases although there has been much theoretical work [20,21].

3.2. Lamellar biogels: multilayer fluid membranes containing membrane-anchored polymer–lipids

Hydrogels of polymer networks constitute a very important class of “soft” matter materials from

both scientific and technological viewpoints. Their uses span diverse areas from the food industry to the medical and biotechnological industries in implants and tissue replacements, drug delivery systems, and bioseparations among others [22–27]. So-called “smart” hydrogels can shrink or expand by a factor of up to 10^3 depending on their local environment have bewildered scientists for over a decade [22,28,29].

As described by Warriner et al. [30] we have recently developed an entirely new class of hydrogels in our laboratory which are based on fluid membranes comprised of lipids and cosurfactants with small amounts of a low molecular weight polymer–lipid PEG–DMPE (Fig. 4). The PEG–lipid is hydrophobically anchored but free to diffuse within the fluid membrane. There are striking differences between these membrane-based liquid crystalline biogels, labeled $L_{\alpha,g}$, and isotropic hydrogels of polymer networks. For example, as the water concentration is increased, a smaller polymer concentration is required for gelation as is seen in the phase diagram (Fig. 5). Furthermore, whereas even concentrated (greater than 50 wt.%) free PEG (molecular weight = 5000)–water mixtures do not gel, gelation occurs in lamellar mixtures containing as little as 0.5 wt.% of PEG (MW = 5000)–lipid. A defining signature of the biogel $L_{\alpha,g}$ regime as it sets in from the fluid lamellar L_{α} phase is the proliferation of defects which are stabilized by the segregation of PEG–lipids to the high membrane curvature defect regions connecting the membranes. The underlying defected structure of these lamellar gels is qualitatively consistent with their unusual macroscopic properties compared with isotropic gels.

Free PEG is a non-ionic water-soluble polymer which has been studied extensively in a broad range of scientifically and technologically important problems in colloidal science and complex fluids [31], and more recently in biology and biotechnology [22]. Because of their extremely low immunogenicity, “free” PEO, a high molecular weight version of PEG, is used to make hydrogels consisting of water-swollen high molecular weight polymer networks in numerous biomedical applications involving tissue replacement [22], and in

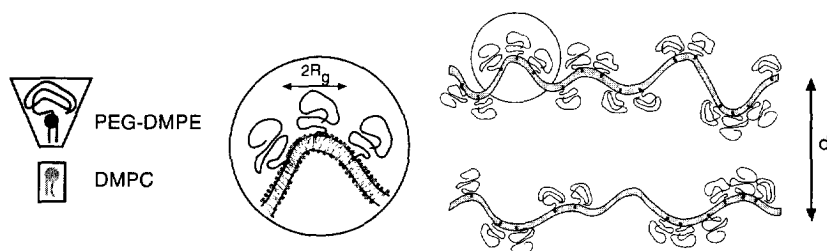


Fig. 4. Schematic diagram of two undulating fluid membranes (comprised of DMPC and cosurfactant pentanol) with PEG–lipid hydrophobically anchored, but freely diffusing within the membrane.

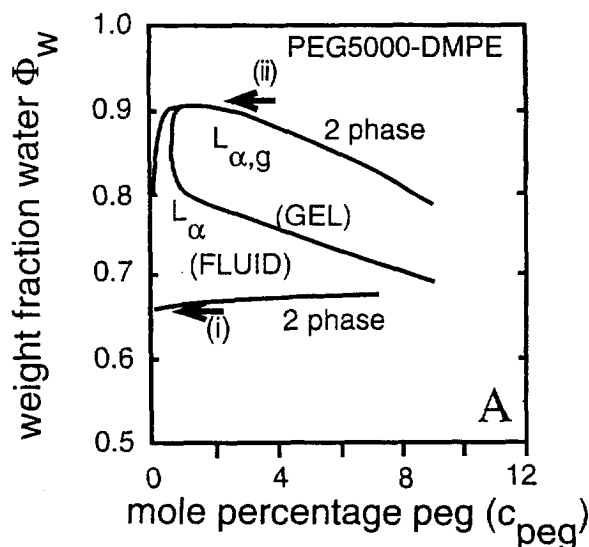


Fig. 5. Phase diagram for single-end-anchored PEG5000–DMPE plotted in terms of the water weight fraction Φ_w vs the mole percentage of PEG–lipid to the total lipid content c_{PEG} . (Redrawn from Warriner et al. [30a].)

synthetic coatings with PEO grafted onto bulk polymeric substances [23].

This immunogenicity has also led to a renaissance in the field of drug and gene delivery applications using liposomes [26]. This is due to the observation of a dramatic increase in blood circulation times in both peptides and proteins protected by covalently attached PEG [27], and in so-called “Stealth” liposomes [24–26] used as a drug carrier system consisting of closed bilayer shells of phospholipids covered with PEG–lipids hydrophobically anchored to the membrane. The inhibition of the body’s immune response to these PEG-

coated liposomes has been attributed [26] to a polymer-brush type steric repulsion [32].

The liquid crystalline biogel is stable in water-swollen lamellar phases with large intermembrane separations $R_g < d < 8R_g$. The $L_{\alpha,g}$ is comprised of membranes of DMPC, the cosurfactant pentanol, and small amounts of the polymer–lipid PEG–DMPE, separated by water. Warriner et al. [30a] described lamellar biogels in two different molecular weights of PEG, 2053 g mol^{-1} (PEG2000) ($n = 45$ is the numbers of monomers) and 5181 g mol^{-1} (PEG5000) ($n = 113$). For both molecular weights of PEG–DMPE, the sample viscosity increases dramatically with the onset of gelation occurring both as a function of increasing PEG–lipid concentration and, unexpectedly, as a function of increasing water concentration as shown in Fig. 6. Normally, lamellar fluid membranes simply show a decrease in viscosity as d is increased at higher water fractions. Here, we find an inverse behavior for gelation, with mixtures of larger water content gelling at smaller PEG–lipid concentrations.

The phase diagram for PEG5000–DMPE showing the L_{α} and $L_{\alpha,g}$ regions is shown in Fig. 5, with the water weight fraction Φ_w plotted versus the mole percentage of PEG–lipid (c_{PEG}) in the total lipid content of the membrane. The radius of gyration of PEG–lipid in lipid membranes has been measured to be about 62 \AA for PEG5000 [33,34]. For $\Phi_w < 0.66$ (see arrow (i) in Fig. 5), which is below the lower two-phase boundary, the stacked bilayers cannot incorporate any PEG5000. This boundary corresponds to an average membrane separation $d_{\text{water}} \approx 60 \text{ \AA}$ ($d = \delta + d_{\text{water}}$, where $\delta = 28 \text{ \AA}$ is the membrane thickness). Thus, as a

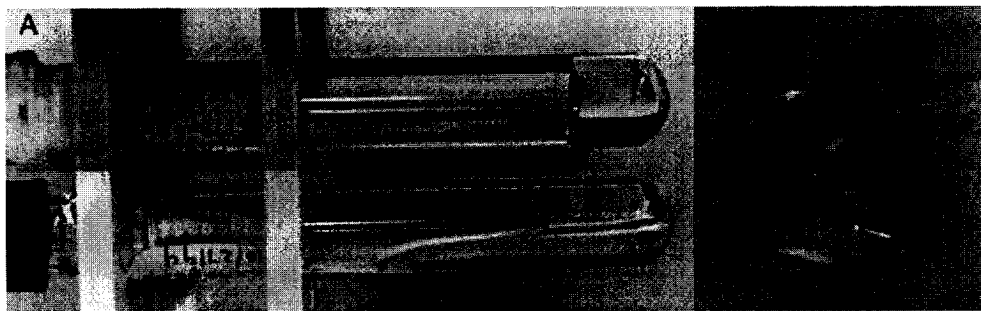


Fig. 6. (A) Two lamellar samples in 13 mm diameter tubes, each with a 6.06 mol% PEG2000–DMPE concentration. Surprisingly, the top bottle, which is a gel, has the larger water content. Lower tube, $\Phi_w=0.45$; top tube, $\Phi_w=0.78$; these correspond to lamellar interlayer spacings $d=55 \text{ \AA}$ and 165.4 \AA . (B) Gel sample (same as top tube in (a)) showing long lived (greater than 6 months) non-spherical bubbles due to the finite yield stress present in the gel. Rheometric measurements of the dynamic elastic moduli show that the elastic storage modulus is much larger than the loss modulus. (From Warriner et al. [30a].)

function of increasing water, the one-phase lamellar region is stable when the separation distance is approximately large enough to accommodate the swollen PEG polymer. The maximum spacings where the lamellar regions remain one phase correspond to $d_{\text{water}} \approx 360 \text{ \AA}$ (see arrow (ii) in Fig. 5) with $d \gg R_g$.

The key difference with previous work [33] which allowed us to explore the regime $d \gg R_g$ where the biogel is stable, was the high flexibility of the fluid membranes within which the PEG–lipid was incorporated. Without PEG–lipid, the addition of the cosurfactant pentanol to membranes consisting of DMPC thins the bilayer membrane which leads to the decrease of its bending rigidity $k \approx k_B T$ [2]. The lamellar L_α phase is then comprised of fluid, highly flexible membranes with interactions dominated by long-range repulsive undulation forces [2,35], giving rise to large inter-membrane distances.

We note that the $L_{\alpha,g}$ phase is a physical gel rather than a traditional chemical gel with permanent covalent bond cross-links [22]. Using approximate values for the PEG radii of gyration [33,34] together with those for the areas of lipid and cosurfactant molecules [2], the concentration where the mushroom-shaped PEG–lipid first covers a flat membrane before any overlap of the polymer chains occurs, is estimated to be about 3 mol% for PEG5000–DMPE. The transition to the gel phase then may occur in PEG–lipid concentrations significantly below the brush regime

(Fig. 5, $\Phi_w > 0.78$), where the polymer does not fully coat the membrane. Thus, the direct interactions between the PEG on opposing layers can be ruled out as a mechanism for gelation.

We show small-angle X-ray powder scans, corresponding to the (001) peaks of the lamellar structure, in four mixtures along a line of increasing PEG2000–DMPE concentration in the fluid (Figs. 7(A) and (B)) and gel (Figs. 7(C) and (D)) regions. Larger-angle experiments verify that the interference peak due to interactions between the lipid chains remains liquid like in both the L_α and $L_{\alpha,g}$ regimes; thus, the addition of PEG–lipid does not affect bilayer fluidity. Hence, unlike L_β , gels, gelation is not due to in-plane chain ordering [36,37]. In a fluid lamellar phase, the onset of the higher harmonics is an indication of the stiffening of the bulk compression modulus B [2,38,39]. This suggests that PEG-coated membranes in a flexible multilayer system experience an enhanced repulsive interaction [40] as a function of increasing c_{PEG} which is consistent with an increase in B . The dramatic transition from fluid to gel is not mirrored in any similarly dramatic change in the X-ray scattering profiles, rather B increases smoothly as c_{PEG} increases. The onset of the harmonics is observed to depend on c_{PEG} , but is essentially independent of the water content Φ_w (or d). Thus, this apparent increase in B is not directly related to the gel transition.

The onset of gelation is marked by a distinct change in the defect structure observed in polarized

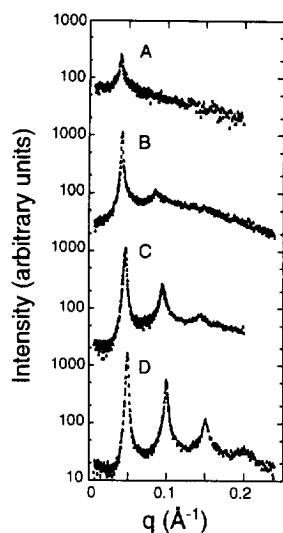


Fig. 7. Synchrotron X-ray scattering data on four samples along an increasing PEG2000–DMPE line: (A) $c_{\text{PEG}}=0$ mol%, $\Phi_w=0.80$, $d=155$ Å; (B) $c_{\text{PEG}}=2.9$ mol%, $\Phi_w=0.78$, $d=147$ Å; (C) $c_{\text{PEG}}=7.8$ mol%, $\Phi_w=0.75$, $d=133$ Å; (D) $c_{\text{PEG}}=15.5$ mol%, $\Phi_w=0.70$, $d=127$ Å. The first two samples are in the L_α fluid and the last two are in the $L_{\alpha,g}$ gel regime which sets in around $c_{\text{PEG}}=4.0 \pm 0.25$ mol%, $\Phi_w=0.76 \pm 0.05$ along this line. (From Warriner et al. [30a].)

light microscopy. Samples in the fluid L_α regime primarily exhibit the typical “oily streak” defects characteristic of lamellar phases with melted chains (Fig. 8(c); x – z plane) shown schematically in Fig. 8(a) (two opposite edge dislocations with large Burgers vectors) [39,41]. As the transition to the $L_{\alpha,g}$ region is approached, we observe a proliferation of defects (Fig. 8(d)). The fluid–gel transition then appears to be driven by the softening of the free energy of defects and their consequent proliferation as observed experimentally.

The gel phase is then characterized by a highly defected microstructure comprised of a network of connected membrane bilayers with the PEG–lipid segregated to the high curvature regions, which on a semimacroscopic length scale leads to random layer orientation domains (Fig. 8(b)). This random layer orientation of domains may lead to elasticity and thus gel-like behavior, because domains which have their layer normals with a finite projection along the flow direction will resist shear, to avoid tilting of layers.

3.3. Entangled tubular vesicles: a new phase of liposomes

Liposomes consist of phospholipids which form closed fluid spheres (because of the hydrophobic effect), capable of encapsulating chemicals. To date, because of their similarities to real cells and their encapsulation properties, liposomes consisting of spherical multilamellar vesicle phases have been extensively studied. From a scientific viewpoint, liposomes are studied as models of interacting cells (e.g. in adhesion and de-adhesion events). From a technological viewpoint, liposomes are currently increasingly utilized in the cosmetics industry (i.e. as a slow chemical release agent) and have potential applications as drug and gene carriers.

The Safinya and Zasadzinski groups at Santa Barbara recently reported on the discovery of a new phase belonging to the family of liposomes consisting of multilamellar tubular vesicles (L_{tv}) [42]. Macroscopic observations (Fig. 9(A) and (B)) show that the L_{tv} is a distinct phase coexisting at equilibrium with the well-known L_4 phase of spherical vesicles and exhibiting under flow the Weissenberg rod climbing effect characteristic of a polymeric-like entanglement for its underlying microstructure. Optical microscopy (shown in Fig. 9(C) and (D)) and electron microscopy reveal it to be liposomes comprised of highly entangled (hollow) tubular vesicles, the L_{tv} phase, in ternary mixtures of DMPC, water and geraniol, a biological cosurfactant derived from oil-soluble vitamins. In-situ X-ray diffraction confirms that the tubule walls are multilamellar with the lipids in the chain-melted state. These tubules are then quite distinct from the solid lipid tubules [43].

This new equilibrium phase of liposomes is not predicted by current theories describing fluid membranes. Among the very dilute phases which appear at equilibrium in surfactant solutions, including the dilute lamellar L_α phases [2] that are stabilized by the Helfrich [35] undulation forces, the equilibrium L_4 phase of spherical vesicles [44,45] and the bicontinuous L_3 phases [46,47], all may be described by considering fluid membranes with physical properties described by Helfrich [35]. In contrast, the existence of the L_{tv} phase is not

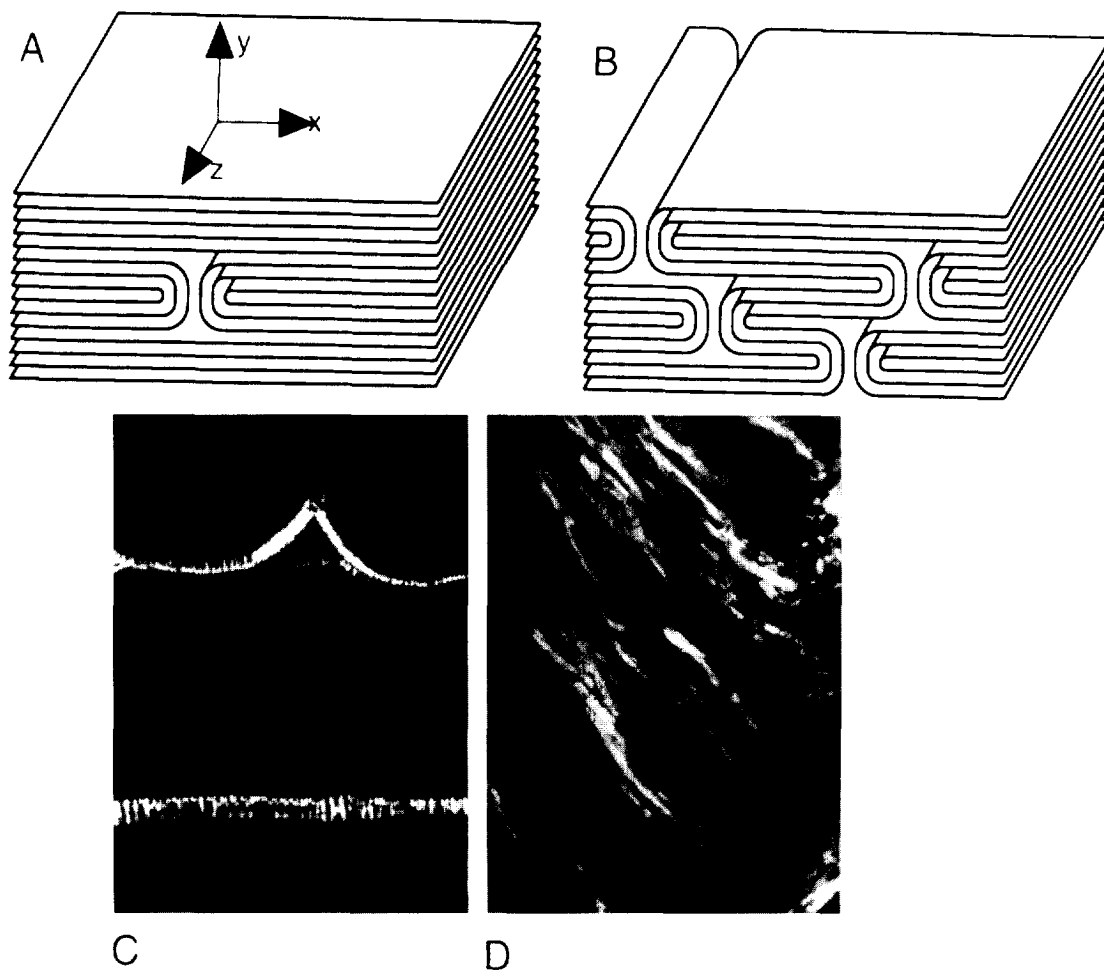


Fig. 8. Real space schematic structure of defects in (A) the fluid L_α and (B) the gel $L_{\alpha,g}$ phases as discussed in the text. Optical microscopy pictures between crossed polarizers of defects in PEG2000-DMPE samples along a line of increasing PEG-lipid concentration (with $\Phi_w + \Phi_{\text{PEG}} = 0.8$). (C) $c_{\text{PEG}} = 1.1$ mol%, $\Phi_w = 0.79$ sample showing the oily streak defects typical of L_α phases. (D) $c_{\text{PEG}} = 4.53$ mol%, $\Phi_w = 0.78$ mixture in the gel phase. The proliferation of defects as the gel phase sets in is evident. (From Warriner et al. [30]a.)

predicted within the Helfrich theory. Recent theoretical work which emphasizes a non-analytical bending energy term that appears to favour cylindrical and “egg-carton” geometries may turn out to be the correct theory of the L_{IV} phase [48].

4. Conclusions

Biomolecular materials are materials that result from research at the interface between materials

science and engineering and biology (see for example [49,50]). This highly interdisciplinary research enterprise claims practitioners from diverse disciplines including soft condensed-matter physics, complex fluids, biophysics, chemical synthesis, biochemistry, molecular cell biology and genetic engineering. In most cases a common structural feature of such materials is self-assembly, in particular, into more highly ordered supramolecular materials.

Among the most interesting biomolecular materi-

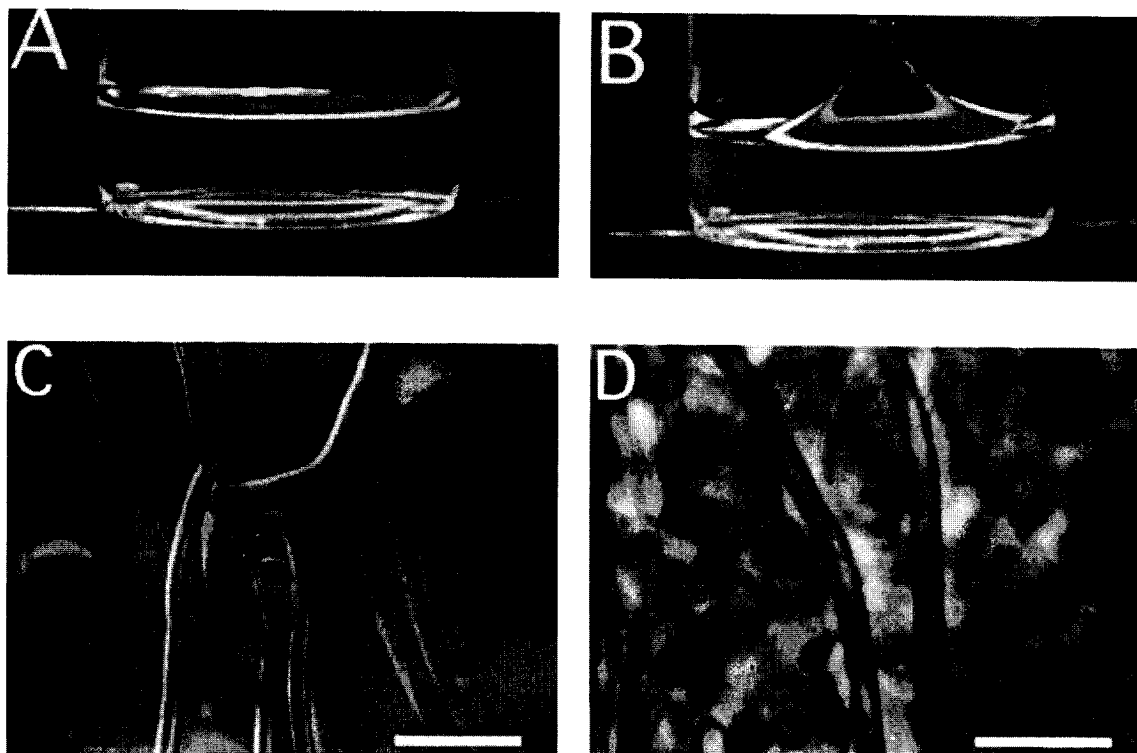


Fig. 9. (A) Photograph of a test-tube showing the interface of a two-phase sample with an upper tubular vesicle phase and a lower dilute spherical vesicle phase. (B) When a rotating rod (not shown) is inserted in the upper phase, the observed response is highly unusual for surfactant solutions: the interface moves inward and upward. This behavior is more commonly observed in entangled polymeric solutions. (C) Optical micrographs using differential interference contrast depicting the multilayered tubular vesicles phase. (D) Phase contrast optical micrograph of a different region of the same sample showing the elongated tubular vesicles. Bars indicate 10 μm . Micrographs taken with a Nikon Diaphot 300. Because of the extremely large structures resolvable by light microscopy, this model polymeric system (of membranes) would allow us to visualize flow-induced distortions of the microstructure of polymeric complex fluids directly. The distortions in turn gives rise to normal stress effects at the macroscopic level which underlie all the technologically useful properties of polymers. (From Chiruvolu et al. [42].)

als are those comprised of self-assembled and functionalized interfaces where the functionality is derived from biomolecules which may be manipulated at the molecular level. For example, 2D self-assemblies of membrane-proteins such as bacteriorhodopsin and similar native bacterial self-assemblies of surface protein layers are of current interest for the development of biomolecular materials in technological areas as diverse as molecular electronics and optical switch applications, to uses as molecular sieves and the lithographic fabrication of nanometre-scale patterns [1, 14, 15]. Functionalized biomolecular interfaces which include receptor proteins could form the basis for developing advanced materials which serve as chemical and biological sensors

[19], or those with controlled interfacial properties such as adhesion and lubrication. In many cases the materials have uses in biomedical applications, e.g. in tissue engineering or in developing self-assembled drug and gene delivery vehicles [26–28].

The fluid membrane-based biogels described in this article [30] immediately suggest new directions for further development of functionalized bioactive materials. Because their principal component is lipid and surfactant, “bioactive gels” useful in tissue healing, in chemical sensing or drug delivery applications [24, 26, 27] may be envisaged with activity derived from membrane-anchored peptides, proteins or other drug molecules, and mechanical stability resulting from the poly-

mer–lipid minority component. By analogy to so-called “smart” hydrogels of polymer networks which respond by contracting or expanding to external stimuli such as temperature, solvent or pH changes [23,29], a suitable choice of lipid and polymer–lipid should lead to a different class of smart lamellar hydrogels.

Bioactive gels may also be envisaged comprised of the reconstitution of bR into the lamellar bio-gels. bR can function as an optically driven bistable switch at low temperatures. Thus, because of the importance of bR in the field of biomaterials research, bR-containing lamellar gels should find much utility. The bioactive gel would combine the optimal mechanical integrity and processability properties of the underlying membrane–polymer structure together with the desirable optical properties of bR.

In the next few years, many researchers of biomolecular materials and complex fluids will almost certainly be working in the area of “non-viral based” gene therapy. Somatic gene therapy depends on the successful transfer and expression of extracellular DNA to the nucleus of eucaryotic cells, with the aim of replacing a defective or adding a missing gene in corrective molecular-level biomedical applications (see for example [51]). While viral-based carriers of DNA are at present the most common method of gene delivery, there has been a tremendous recent surge in activity in the development of synthetically based non-viral vectors. In particular, an important recent breakthrough involves the use of cationic liposomes (CL) as non-viral transfer vectors (i.e. carriers) of recombinant DNA molecules [52]. While significantly improved in transfection efficiency compared with other non-viral carriers, at present, CL vectors exhibit much lower efficiencies than do viral vectors. This low efficiency is related to the lack of fundamental knowledge regarding the mechanisms which underly transfection via “cationic” liposomes [51–53]. In particular, what is the precise nature of the interactions and resulting structures of the CL–DNA complexes? What are the interactions of the complex with intracellular organelles and the mechanism of transfer across the nuclear membrane? Recent experiments are now beginning to address properly the structure

of the complexes through quantitative X-ray diffraction studies which are revealing a well-defined, more highly ordered liquid crystalline structure of the CL–DNA complexes with the DNA, which is intercalated between cationic lipid bilayers, forming a well-defined one-dimensional lattice of DNA chains [54].

The obvious complexity in biomolecular materials research makes the field especially pleasing because of the seemingly unlimited number of very important unresolved problems. Furthermore, while almost no problem in this area will be completely solved owing to its complexity, because of the importance of the field, even small progress towards their solution tends to lead to large gains from scientific, technological, medical and environmental aspects.

Acknowledgment

Philip Pincus is especially acknowledged for collaboration and countless beneficial discussions on biomaterials. Jean-Louis Rigaud and Joe Zasadzinski are thanked for recent collaboration related to biomaterials. Hollis Wickman (National Science Foundation) is thanked for his constant encouragement of research on biomolecular materials. We would like to acknowledge the close collaboration with Ken Rothschild’s group which focuses on the biomaterials aspects of bR mutants obtained through the latest methods of recombinant DNA. Robijn Bruinsma, Bill Gelbart, Devarajan Thirumalai, Tom Lubensky, David Morse and David Nelson are thanked for relevant conversations. Very importantly, the collaboration of research members in the Safinya group working on biomaterials is acknowledged including Patrick Davidson, Stefan Idziak, Ilya Koltover, Alison Lin, Joachim Raedler, Tim Salditt, Nelle Slack, Subu Subramanian and Heidi Warriner. The work was partially supported by National Science Foundation grant DMR-9624091, the Petroleum Research Fund (Grant 31352-AC7), a Los Alamos CULAR Grant STB/UC:95-146 and a Los Alamos-UC Campus Collaborative Research Initiative under Award UC-94-8-A-221. The Materials Research Laboratory at Santa Barbara

is supported by National Science Foundation Grant DMR 96-32716. The synchrotron experiments were carried out at Stanford Synchrotron Radiation Laboratory and the National Synchrotron Light Source, which are supported by the US Department of Energy.

References

- [1] W. Baumeister, H. Engelhardt, in: J.R. Harris, R.W. Horne (Eds.), *Electron Microscopy of Proteins*, vol. 6, Academic Press, London, 1987, p. 109; W. Baumeister, W. Vogell (Eds.), *Electron Microscopy at Molecular Dimensions: State of the Art and Strategies for the Future*, Springer, Berlin, 1980; N. Unwin, R. Henderson, *Sci. Am.* February (1984).
- [2] C.R. Safinya, in: T. Riste and D. Sherrington (Eds.), *Phase Transitions in Soft Condensed Matter*, in NATO Adv. Stud. Inst. Ser., Ser. B, 211 (1989) 249; C.R. Safinya et al., *Phys. Rev. Lett.* 57 (1986) 2718; C.R. Safinya, E.B. Sirota, D. Roux, G.S. Smith, *Phys. Rev. Lett.* 62 (1989) 1134; G.S. Smith, E.B. Sirota, C. Safinya, R.J. Plano, N.A. Clark, *J. Chem. Phys.* 92 (1990) 4519; D. Roux, C.R. Safinya, F. Nallet, in: A. Ben-Shaul, W.M. Gelbart, D. Roux (Eds.), *Micelles, Membranes, Microemulsions and Monolayers*, Springer, New York, 1994.
- [3] C.F. Schmidt, K. Svoboda, N. Lei, I. Petsche, L. Berman, C.R. Safinya, and G.S. Grest, *Science* 259 (1993) 952; S.H.J. Idziak, C.R. Safinya, R.S. Hill, M. Ruth, H.E. Warriner, K.E. Kraiser, K.S. Liang, J.N. Israelachvili, *Science* 264 (1994) 1915; S. Chiruvolu, H.E. Warriner, E. Naranjo, K. Kraiser, S. Idziak, J. Radler, R.J. Plano, J.A. Zasadzinski, C.R. Safinya, *Science* 266 (1994) 1222; B.N. Thomas, C.R. Safinya, R.J. Plano, N.A. Clark, *Science* 267 (1995) 1635.
- [4] C.R. Safinya, Yi Shen, in: T. Riste, D. Sherrington (Eds.), *Physics of Biomaterials: Fluctuations, Self-Assembly, and Evolution*, in NATO Adv. Stud. Inst. Ser., Ser. E, 322 (1996) 103–134; Y. Shen, C.R. Safinya, I. Koltover, J. Raedler, B.N. Thomas, N.A. Clark, K.J. Rothschild, to be submitted.
- [5] P.M. Eisenberger, L.C. Feldman, *Science* 214 (1981) 300; I.K. Robinson, in: D.E. Moncton (Ed.), *Handbook on Synchrotron Radiation*, vol. 3, North-Holland, Amsterdam, 1987; D.E. Moncton, G.S. Brown, *Nucl. Instrum. Methods* 208 (1983) 579; R.J. Birgeneau, P.M. Horn, *Science* 232 (1986) 329; D. Gibbs, B.M. Ocko, D.M. Zehner, S.G.J. Mochrie, *Phys. Rev. B* 42 (1990) 7330.
- [6] J. Als-Nielsen, in *Top. Curr. Phys.*, 43 (1987) 181; P.S. Pershan, *J. Phys. (Paris)* 50, Coll. C7 (1989) s1.
- [7] S.K. Sinha, E.B. Sirota, S. Garoff, H.B. Stanley, *Phys. Rev. B* 38 (1988) 2297.
- [8] Yi Shen, C.R. Safinya, K.S. Liang, A.F. Ruppert, K.J. Rothschild, *Nature* 366 (1993) 48; N. Hampp, *Nature* 366 (1993) 12; *Chem. Eng. News* November 8 (1993) 40.
- [9] C.R. Safinya, K.J. Rothschild, *Nature* 370 (1994) 105.
- [10] T.D. Brock, M.T. Madigan, *Biology of Microorganisms*, 6th ed., Prentice Hall, Englewood Cliffs, NJ, 1991; C.R. Woese, *Sci. Am.* June (1981).
- [11] D. Oesterhelt, W. Stoekenius, *Nature New Biol.* 233 (1971) 149; *Proc. Nat. Acad. Sci. USA* 70 (1973) 2853; W. Stoekenius, *Sci. Am.* June (1976) 38; A.E. Blaurock, W. Stockenius, *Nature New Biol.* 233 (1971) 152.
- [12] R. Henderson, P.N.T. Unwin, *Nature* 257 (1975) 28.
- [13] M.S. Braiman, K.J. Rothschild, *Ann. Rev. Biophys. Biophys. Chem.* 17 (1988) 541.
- [14] M. Dunach, S. Berkowitz, T. Marti, Y.W. He, S.J. Subramaniam, et al. *Biol. Chem.* 265 (1990) 16 978; P.L. Ahl, L.J. Stern, T. Mogi, H.G. Khorana, K.J. Rothschild, *Biochemistry* 28 (1989) 10 028.
- [15] N. Hampp, C. Brauchle, D. Oesterhelt, *Biophys. J.* 58 (1990) 83.
- [16] T. Gulik-Krzywicki, M. Seigneuret, J.-L. Rigaud, *J. Biochem.* 262 (32) (1987) 15 580; N.A. Dencher, K.D. Kohl, M.P. Heyn, *Biochemistry* 22 (1983) 1323.
- [17] Uzgiris, Kornberg, *Nature* 301 (1983) 125.
- [18] N.M. Green, *Adv. Protein Chem.* 29 (1975) 85.
- [19] D. Leckband, *Nature* 376 (1995) 617 and references cited therein; M. Wilcheck, E.B. Bayer (Eds.), *Avadin-Biotin Technology, Methods in Enzymology*, vol. 184, Academic Press, New York, 1989.
- [20] N. Dan, P. Pincus, S.A. Safran, *Langmuir* 9 (1993) 2768; N. Dan, A. Berman, P. Pincus, S.A. Safran, *J. Phys. (Paris)* II 4 (1994) 1713.
- [21] M. Goulian, R. Bruinsma, P. Pincus, *Europhys. Lett.* 22 (1993) 145; R. Bruinsma, M. Goulian, P. Pincus, *Biophys. J.* 6 (1994) 746; K.M. Palmer, M. Goulian, P. Pincus, *J. Phys. (Paris)* II 4 (1994) 805.
- [22] D. DeRossi, K. Kajiwara, Y. Osada, A. Yamauchi, *Polymer Gels: Fundamentals and Biomedical Applications*, Plenum Press, 1991.
- [23] N.A. Peppas, R. Langer, *Science* 263 (1994) 1715.
- [24] T.M. Allen, A. Chonn, *FEBS Lett.* 223 (1987) 42; A. Gabizon, D. Papahadjopoulos, *Proc. Nat. Acad. Sci. USA* 85 (1988) 6949.
- [25] D.D. Lasic, in: *Liposomes: From Physics to Applications*, Elsevier, Amsterdam, 1993.
- [26] D.D. Lasic, D. Papahadjopoulos, *Science* 267 (1995) 1275; D.D. Lasic, F.J. Martin (Eds.), *Stealth Liposomes*, CRC Press, Boca Raton, FL, 1995.
- [27] V.H.L. Lee (Ed.), *Peptide and Protein Drug Delivery*, Dekker, New York, 1991.
- [28] F. Ilmain, T. Tanaka, E. Kokufuta, *Nature* 349 (1991) 400; E.S. Matsu, T. Tanaka, *Nature* 358 (1992) 482.
- [29] Y. Osada, S.B. Ross-Murphy, *Sci. Am.* 268 (1993) 82; Z. Hu, X. Zhang, Y. Li, *Science* 269 (1995) 525.
- [30] (a) H.E. Warriner, S.H.J. Idziak, N.L. Slack, P. Davidson, C.R. Safinya, *Science* 271 (1996) 969; (b) B. Hanson (Ed.), *This Week In Science*, *Science* 271 (1996) 969.

- [31] F.E. Bailey, Jr., J.V. Koleske, Poly(ethylene oxide), Academic Press, New York, 1976.
- [32] S. Alexander, *J. Phys. (Paris)* 38 (1977) 977; P.-G. De Gennes, *J. Phys. (Paris)* 37 (1976) 1443; P.-G. De Gennes, *Macromolecules* 13 (1980) 1069; S.T. Milner, *Science* 251 (1991) 905; G. Subramanian, D.R.M. Williams, P.A. Pincus, *Europhys. Lett.* 29 (1995) 285.
- [33] D. Needham, T.J. McIntosh, D.D. Lasic, *Biochim. Biophys. Acta* 1108 (1992) 40; A.K. Kemworthy, K. Hristova, D. Needham, T.J. McIntosh, *Biophys. J.* 68 (1995) 1921.
- [34] T.L. Kuhl, D.E. Leckband, D.D. Lasic, J.N. Israelachvili, *Biophys. J.* 66 (1994) 1479.
- [35] W. Helfrich, *Z. Naturforsch.* 33a (1978) 305; 28c (1973) 693.
- [36] M.J. Janiak, D.M. Smalley, G.G. Shipley, *J. Biol. Chem.* 254 (1979) 6068.
- [37] G.S. Smith, E.B. Sirota, C.R. Safinya, N.A. Clark, *Phys. Rev. Lett.* 60 (1988) 813; G.S. Smith, E.B. Sirota, C.R. Safinya, R.J. Plano, N.A. Clark, *J. Chem. Phys.* 92 (1990) 4519.
- [38] N. Lei, C.R. Safinya, R. Bruinsma, *J. Phys. (Paris) II* 5 (1995) 1155.
- [39] P.-G. De Gennes, J. Prost, *The Physics of Liquid Crystals*, 2nd ed., Clarendon Press, Oxford, 1993.
- [40] H.E. Warriner, C.R. Safinya, P. Pincus, to be submitted.
- [41] S.A. Asher, P.S. Pershan, *Biophys. J.* 27 (1979) 393; M.B. Schneider, W.W. Webb, *J. Phys. (Paris)* 45 (1984) 273.
- [42] S. Chiruvolu, H.E. Warriner, E. Naranjo, K. Kraiser, S.H.J. Idziak, J. Radler, R.J. Plano, J.A. Zasadzinski, C.R. Safinya, *Science* 266 (1994) 1222; P. Szuromi (Ed.), *This Week In Science*, *Science* 266 (1994) 1222.
- [43] B.N. Thomas, C.R. Safinya, R.J. Plano, N.A. Clark, *Science* 267 (1995) 1635; M.E. Davis, *Nature* 364 (1993) 391; D.D. Archibald, S. Mann, *Nature* 364 (1993) 430; R. Baum, *Chem. Eng. News* August 9 (1993) 19.
- [44] E.W. Kaler, A.K. Murthy, B.E. Rodriguez, J.A.N. Zasadzinski, *Science* 245 (1989) 1371.
- [45] S.A. Safran, P. Pincus, D. Andelman, *Science* 248 (1990) 354.
- [46] G. Porte, J. Marignan, P. Bassereau, R.J. May, *J. Phys. (Paris)* 49 (1988) 511.
- [47] M.E. Cates, D. Roux, D. Andelman, S.T. Milner, S.A. Safran, *Europhys. Lett.* 5 (1988) 733.
- [48] J.B. Fournier, *Phys. Rev. Lett.* 76 (1996) 4436.
- [49] Rep. of the University/Industry Workshop¹, US National Science Foundation Rep. NSF 91-142, 1990.
- [50] C.R. Safinya, L. Addadi, *Curr. Opin. Solid State Mater. Sci.* 1 (1996) 387–391.
- [51] A. Singhal, L. Huang, in: J.A. Wolff (Ed.), *Gene Therapeutics: Methods and Applications of Direct Gene Transfer*, Birkhauser, Boston, MA, 1994.
- [52] P.L. Felgner, et al., *Proc. Nat. Acad. Sci. USA*, 84 (1987) 7413; P.L. Felgner, G. Rhodes, *Nature* 349 (1991) 351.
- [53] *Science* 269 (1995) 1050–1055.
- [54] J.O. Radler, I. Koltover, T. Salditt, C.R. Safinya, *Science* (1997) 275 (1997) 810–814.

¹ The words “biomolecular materials” were first introduced at this workshop by H. Hollis Wickman of the National Science Foundation.